Boosting Respiratory Immunity with Nasal Commensals and Advancing a Novel Recombinant Vaccine Against *Bordetella Pertussis* Infection

Da Jung Kim

Department of Medical Science

The Graduate School, Yonsei University

Boosting Respiratory Immunity with Nasal Commensals and Advancing a Novel Recombinant Vaccine Against *Bordetella Pertussis* Infection

Directed by Professor Ho-Keun Kwon

The Master's Thesis
submitted to the Department of Medical Science,
the Graduate School of Yonsei University
in partial fulfillment of the requirements for the degree of
Master of Medical Science

Da Jung Kim

December 2023

This certifies that the Master's Thesis
of Da Jung Kim is approved.

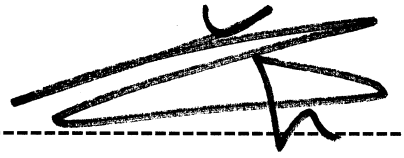

Thesis Supervisor : Ho-Keun Kwon

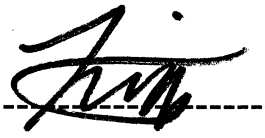

Thesis Committee Member#1 : June-Yong Lee

Thesis Committee Member#2 : Ji-Heui Kim

The Graduate School
Yonsei University

December 2023

ACKNOWLEDGEMENTS

논문을 마무리 하는 날이 다가올 줄 몰랐는데, 한 걸음 사이에 졸업하는 날이 가까워 짐이 실감 나고 있습니다. 처음 권랩에 들어올 때만 해도 갓 졸업한 대학생이었지만, 이제는 20대 후반을 달리고 있는 어른이 되었네요. 어쩌면 20대 인생의 가장 중요한 시기이자 크게 성장할 수 있는 기회였다고 생각합니다. 훌쩍 다가온 졸업에는 역시 제 주변 사람들의 큰 역할이 있었기에 가능했습니다.

가장 먼저 따끔한 조언부터 무한한 가르침까지, 무지했던 저를 크게 성장시켜 주신 권호근 교수님께 감사하다는 말씀 전하고 싶습니다. 늘 부족한 학생이었지만 큰 가르침 덕분에 많이 배울 수 있었습니다. 또한, 연구의 방향성과 더 나은 연구를 해줄 수 있게 도와 주신 이준용 교수님과 김지희 교수님께도 정말 감사합니다. 그리고 제 대학원 삶에 없어서는 안될 분이신 김기천 박사님께도 감사합니다. 덕분에 많은 실험을 배울 수 있었고 곁에서 응원해 주시며 큰 도움을 주셨습니다. 그 외에도 아낌없는 조언을 주신 최주리 박사님, 장이정 박사님께도 감사드립니다.

항상 제 주변에는 좋은 사람들이 있었고, 그 중 3년의 시간을 가장 오랫동안 같이 보낸 해원이에게 감사합니다. 해원이는 긴 대학원 생활의 친구이자, 든든한 조력자 역할을 해줬습니다. 그 외에도 졸업하신 두 연수, 수빈 선배님들, 모르는 게 있을 때마다 자문을 구하고 철 없는 동생을 올바른 길로 안내해주며 인생 선배 역할을 해준 똑똑한 종휘쌤, 옆 자리에서 높은 데시벨과 칭얼거림을 받아준 착한 준수쌤, 나의 인턴 동기인 밝은 여진쌤, 자라나는 새싹들인 시윤쌤, 정진쌤, 승준쌤 등 랩실 원 모두에게 감사합니다. 또한, 부모님의 든든한 지원과 사랑이 없이는 버티기 힘들었을 겁니다.

바쁘다는 핑계로 자주 찾아 뵙지 못했지만, 졸업한 후에는 얼굴 자주 보면서 효도하도록 하겠습니다. 항상 감사한 마음 가지고 있습니다.

마지막으로, 마음 잘 맞는 내 307 친구들, 입학부터 졸업까지 정신적 지주 역할을 해준 창현이에게 감사합니다. 그 외에도 주변 사람들의 많은 응원과 격려 또한 모두 감사합니다. 드디어 졸업 후 새로운 출발을 향해 나아갑니다! 화이팅!

TABLE OF CONTENTS

LIST OF FIGURES

ABSTRACT

Boosting Respiratory Immunity with Nasal Commensals and Advancing a Novel Recombinant Vaccine Against *Bordetella Pertussis* Infection

Da Jung Kim

Department of Medical Science
The Graduate School, Yonsei University

(Directed by Professor Ho-Keun Kwon)

Whooping cough caused by *Bordetella pertussis* (*B. pertussis*) is a contagious respiratory tract disease. Acellular pertussis (aP) vaccines were developed as a replacement for whole-cell pertussis (wP) vaccines, which contain inactivated pertussis toxin (PTX) and other bacterial components, filamentous hemagglutinin (FHA) and pertactin (PRN). However, whooping cough outbreaks occurred in aP-vaccinated populations because of the limited and transient T helper 1 (Th1) / T helper 17 (Th17)-mediated immunogenicity of aP vaccines as well as their propensity to generate T helper 2 (Th2)-biased immune responses. To overcome the limitations of these aP vaccines, we developed two promising strategies: (1) administering nasal commensals to protect the host against respiratory pathogens through mucosal immune boosting and (2) developing novel recombinant aP (NRaP) vaccines based on recombinant pertussis proteins.

Nasal commensals reside in the upper respiratory mucus layer, which is the first line of defense and acts as a gatekeeper of the respiratory tract. The respiratory microbiome protects the host through direct competition with pathogens and indirectly modulates innate and adaptive immune responses. Bacteria that are frequently found in nasal mucosal niches are *Staphylococcus* species. *Staphylococcus epidermidis* (*S. epidermidis*) is a representative microbiota that restricts opportunistic pathogen invasion by secreting serine proteases or inducing proinflammatory cytokine production by stimulating the nasal epithelium. To investigate the immunological properties of this bacterium, we inoculated *S. epidermidis* and identified its antimicrobial effects using a *B. pertussis* infection mouse model. We revealed that *S. epidermidis* enhances the IL-17a^{+} mediated immune responses and suppresses *B. pertussis* colonization in acute infection.

We have engineered a novel subunit pertussis vaccine by introducing pertussis antigens into competent cells, aiming to boost the immunogenicity of current aP vaccines. Mice immunized with this new vaccine, ChaH2-Prn, exhibited higher titers of Prn-specific IgG antibodies compared to those immunized with the conventional aP vaccines. Moreover, mice vaccinated with our NRaP vaccine demonstrated a reduced bacterial load in the lungs following *B. pertussis* infection, indicating an enhanced protective response.

Furthermore, our research has shed light on the antibacterial properties of nasal commensals that activate mucosal immunity and offer immediate defense against bacterial pathogens. By improving upon the NRaP vaccines, we have addressed the shortcomings of current aP vaccines and introduced a promising approach for bolstering immunogenicity to prevent *B. pertussis* infections.

Key words: respiratory immunity, vaccine, respiratory infection, nasal commensals

Boosting Respiratory Immunity with Nasal Commensals and Advancing a Novel Recombinant Vaccine Against *Bordetella Pertussis* Infection

Da Jung Kim

Department of Medical Science
The Graduate School, Yonsei University

(Directed by Professor Ho-Keun Kwon)

I. INTRODUCTION

Respiratory tract infections (RTIs) are a significant global health concern, with continuous occurrences of influenza and the emergence of COVID-19 associated with high morbidity and mortality. Various studies have been extensively conducted to prevent respiratory infections, and this study aimed to prevent the recurrence of the respiratory pathogen *B. pertussis. B. pertussis* is a causative agent that leads to whooping cough, a respiratory illness that can cause life-threatening complications in babies[1]. *B. pertussis* attaches to epithelial cells in the lung using the virulence factors FHA, PTX, and PRN[2,3]. These factors disrupt the epithelium and activate resident immune cells, resulting in systemic inflammation. In response to acute *B. pertussis* infection, epithelial cells secrete antimicrobial peptides, cytokines, and chemokines, which recruit neutrophils and macrophages to the infection site[4,5]. A recent study showed a robust increase in transcripts involved in innate immune activation, such as CXCL8 and IL-6, using *B. pertussis*-infected

primary human airway epithelium cells[6]. At 4 days post-infection in mouse lung, innate immune cells are activated, following pathogen recognition, antigen presentation, and phagocytosis in the killing of bacteria. *B. pertussis* further induces Th1 and Th17 cells and upregulates Th1/Th17 cytokines such as interferon-gamma (IFN-γ) and IL-17 within 14 days after infection[5,7]. Mice deficient in IFN-γ and IL-17 showed a higher bacterial burden in the lung and nasopharynx, indicating that Th1 and Th17 cells are the critical T cell subset for protective immunity in response to *B. pertussis*[7,8]. Simultaneously, pertussis-specific IgA and IgG levels were elevated in the serum and lungs, indicating that humoral immune responses were observed in both the systemic and local environment[9]. *B. pertussis* infection also leads to the expansion of $CD4^+$ tissue-resident memory T (Trm) cells as well as γδ Trm cells, which contribute an important role in the clearance of re-infection of the bacteria[4,8,10]. These findings indicate that elevated cellular and antibody-mediated immune responses and prolonged immunity are essential for *B. pertussis* clearance.

In the early 20^{th} century, a wP vaccine containing all inactivated pertussis organisms was developed[11]. Although the wP vaccine reduced the incidence of whooping cough, it had significant adverse side effects, such as high fever, and even caused infant deaths. Thus, an aP vaccine was developed as a replacement for the wP vaccine, which is composed of purified pertussis virulence factors (FHA, PTX, PRN) formulated with alum hydroxide as an adjuvant[12]. However, aP vaccination showed a predominant Th2-biased immune response and short-term immunogenicity[13,14]. Recent work has suggested that the immune responses of individuals who received initial doses of aP vaccines showed remarkably high type 2 polarized pertussis-specific memory $CD4^+$ T cell[13]. Moreover, repeated booster doses of aP vaccine in children primed with acellular vaccine have been shown to result in a progressively shorter duration of protection [15]against disease. Lastly, the aP vaccine induces less immunogenicity than the wP vaccine due to the chemically inactivated toxin; therefore, its replacement is accompanied by an increased incidence of whooping cough and a waning of immunity[13]. In addition, genetic polymorphisms of *B. pertussis* virulence

antigens increased the resistance of the aP vaccine and ultimately failed to prevent *B. pertussis* infection, indicating that the aP vaccine alone is insufficient to eradicate the bacterial infection[16,17]. Thus, there is a growing need for new and improved strategies beyond vaccine enhancement and development.

The nasal epithelium is the first line of defense against inhaled pathogens that cause upper and lower respiratory tract infection[18]. Respiratory commensal bacteria reside in the mucosal barrier and protect the host from pathogen invasion. These commensals act as gatekeepers and sustain mucosal immune homeostasis by promoting local immune responses[19,20]. Thus, a balanced microbiota composition in the upper respiratory tract (URT) is critical for host protection against infection by opportunistic pathogens. According to prior studies, the diversity of bacterial communities in the oropharynx typically declined with increasing disease severity, especially COVID-19, suggesting that the balanced abundance of the URT microbiome is associated with RTIs.[21] We investigated the beneficial role of the microorganism *Staphylococcus epidermidis* (*S. epidermidis*), which is a representative commensal found in the nasal middle turbinate, accounting for ~35% of the identified bacterial species in healthy human nasal mucus[22,23]. Research on *S. epidermidis* has focused on a commensal microorganism that colonizes the skin[24]. However, some studies have recently elucidated its role as a nasal commensal. Previous studies have demonstrated the immunological defensive mechanism of *S. epidermidis,* which attenuates H1N1 influenza virus entry into the nasal mucosa by stimulating an IFN-λ-dependent antiviral response[23]. In addition, *S. epidermidis* triggers antimicrobial peptide production, such as LL-37 and hBD3, by stimulating nasal keratinocytes and outcompetes pathogenic bacteria by forming biofilms[22]. Consequently, these results suggest that nasal commensal *S. epidermidis*-mediated suppression of pathogen outgrowth and mucosal immune boosting contribute to host protection against *B. pertussis* infection.

In this study, we aimed to present two possibilities for preventing infection against *B.*

pertussis: (1) administration of nasal commensal, which could defend the host against pathogens with immunomodulatory properties, and (2) development of new pertussis vaccines to induce sufficient and herd immunity. In part 1, we first investigated the immunological effects of *S. epidermidis* in the nasal cavity *in vivo* and its protective effects against *B. pertussis* infection. We identified that intranasal inoculation with *S. epidermidis* highly activates mucosal immunity, especially IL-17a-expressing immune cells, which are important for killing extracellular bacteria. *S. epidermidis* protects the respiratory tract against acute *B. pertussis* infection *in vivo*. Administration of *S. epidermidis* before *B. pertussis* challenge reduced the bacterial burden in the mouse lung compared with the non-*S. epidermidis*-administered group. In the case of *B. pertussis* infection, there was a decrease in IL-17a-producing $CD4^+$, $CD8^+$, and γδ T cells in the nasal tissue. However, *S. epidermidis* inoculation acted as a type 17 immune booster in these cell types, ultimately preventing *B. pertussis* infection in advance. Our results suggest that pre-treatment with *S. epidermidis* is a promising strategy for protecting the host against respiratory tract infection.

In part 2, we developed recombinant pertussis proteins by using the glutamyl-prolyl-tRNA synthetase which is called 'Chaperna Human 2' (ChaH2). ChaH2 was used as a fusion partner to reduce protein misfolding and insolubility. In contrast to commercial aP vaccines, in which the PTX genes undergo chemical detoxification methods, our approach involves genetic modification to induce higher immunogenicity. The purified pertussis virulence factors were transformed into competent cells that maintained high expression levels of nontoxic recombinant proteins. In the case of the PRN antigen, a higher level of antigen-specific IgG response was observed in mice immunized with the NRaP vaccine than the commercial aP vaccine. In addition, NRaP vaccine-immunized mice exhibited significantly lower pathogenesis upon *B. pertussis* infection than non-immunized mice, representing high vaccine immunogenicity. In summary, our research has uncovered novel strategies for the prevention of respiratory infections, highlighting the potential of NRaP vaccines and nasal commensals to act synergistically as natural adjuvants

MATERIALS AND METHODS

1. Animals

Wild-type C57BL/6(J) mice were purchased from Orient Bio (Sungnam, Korea) and maintained under the Avison Biomedical Research Center (ABMRC) Animal Research Center at Yonsei University College of Medicine, a specific pathogen-free (SPF) facility. All mouse experiments were conducted according to the guidelines of the Animal Research Committee of Yonsei University. The guidelines were approved by the Association for Assessment and Accreditation of Laboratory Animal Care.

2. Bacteria culture

S. epidermidis was grown on tryptic soy agar (TSA) plates and cultured overnight at 37℃. Bacteria were collected in 3 ml tryptic soy broth (TSB) and cultured overnight at 37℃. OD was measured at 600 nm. *B. pertussis* bacteria were grown on a Bordet- Gengou agar (BGA) plate containing 10% glycerol, 15% defibrinated horse blood, and 1% Bordetella supplement at 37℃. After 7 days of culture, the bacteria were sub-cultured on fresh BGA plates and incubated for 7 days. Bacteria were collected, and the OD was measured at 600 nm.

3. Inoculation of *S. epidermidis*

S. epidermidis was inoculated intranasally for 5 consecutive days with CFU as described above. To identify *S. epidermidis* colonization, the nasal wash was collected in phosphate-buffered saline (PBS) by vortexing nasal tissues and spread on a mannitol salt agar (MSA) plate overnight at 37℃.

4. Isolation and flow cytometry analysis of cells isolated from nasal tissue

Nasal tissue, including the nasal cavity and nasal turbinate, was obtained by cutting down the vertical plane of the skull and scraping out the tissues and small bones from both sides of the nasal passages. Nasal tissues were enzymatically digested for 15 min at 37℃ in 1ml of digestion buffer containing collagenase type II (Gibco, 17101015) (3mg/ml) in RPMI 1640 supplemented with 2% Fetal Bovine Serum (Gibco, A4766801). Digested tissues were passed through a 100 μm cell strainer and dissociated into single-cell suspensions. To detect intracellular cytokines, cells were stimulated with 1X stimulation cocktail containing protein transport inhibitors (Invitrogen, 00-4970-03) for 4 h at 37℃ in 5% CO_2. After stimulation, cells were washed and stained for 30 min at 4℃ with the mixture of fluorescent-conjugated monoclonal antibodies. Cells were fixed overnight at 4℃ and permeabilized in the 1X permeabilization buffer (Invitrogen, 00-5523-00). To detect intracellular markers, cells were stained for 20 min at room temperature with a mixture of fluorescent-conjugated monoclonal antibodies. Cells were resuspended in 200 μl PBS and analyzed by multi-color flow cytometry using a SONY ID7000 spectral cell analyzer.

5. *B. pertussis* respiratory challenge

For *B. pertussis* infection, 6-week-old C57BL/6(J) mice were anesthetized by intraperitoneal injection with a mixture of ketamine (50mg per kilogram of body weight) and rumpun (5mg per kilogram of body weight). Cultured *B. pertussis* was inoculated at 8×10^8 CFU per 40 μl into the nasal cavity of mice. Mice were perfused with 20 ml of PBS, and lung tissues were dissected into four lobes for pathological (histology) examination and bacterial load analysis (RT-PCR, culture).

1) Histology

Lungs were washed with PBS and fixed with 4% paraformaldehyde (PFA) for 24 h at 4℃. Tissues were washed twice with PBS and placed on a cassette in 4% PFA. Paraffin-embedded lung tissues were sectioned into 4-μm sections and stained with Hematoxylin and Eosin (H&E). Lung sections were scored in a single-blinded fashion under a light microscope to determine the degree of inflammation in the alveoli and surrounding vessels. Slides were evaluated using 1-4 scoring system, which was 0 (normal), 1 (mild inflammation), 2 (moderate inflammation), 3 (marked inflammation), and 4 (severe inflammation)[25,26].

2) Colony-forming unit (CFU) counting

To determine the bacterial load, divided mice lungs were sonicated in PBS (10% amplitude, 45 seconds) and serial dilutions were spotted on the BGA plate. The plate was incubated at 37℃ for 7 days, and bacterial counts were assessed by log 10 of CFU/lungs.

3) Quantitative Real-time PCR (qRT-PCR)

Total lung genomic DNA (gDNA) was extracted using gDNA extraction buffer with protease K (sigma, p4850) at 55℃ for 12 h. After phenol-chloroform extraction, 70% ethanol was added to the samples and centrifuged twice. Extracted gDNA was eluted with RNase-free water. RT-PCR was performed using SYBR™ Green PCR Master Mix (Thermo-fisher, 4309155), and relative expression levels were analyzed using the QuantStudio3 Real-Time PCR System.

6. Mouse immunization

Infanrix-IPV [GlaxoSmithKline (GSK)] was used as the commercially available aP vaccine. The pertussis recombinant proteins ChaH2-PtxA^{m}, ChaH2-FhaB, and ChaH2-Prn were prepared at the same dose of Infanrix. The recombinant antigens were diluted in sterile PBS with containing alum hydroxide (Invivogen, 21645-51-2), and a final dose of 50 μl was injected intramuscularly. For the control group, mice were immunized with PBS containing alum hydroxide. Mice were anesthetized using a mixture of ketamine (50mg per kilogram of body weight) and rumpun (5mg per kilogram of body weight) and injected intraperitoneally. Following an immunization schedule of priming at week 0 and boosting at week 2, serum samples were collected at week 4 via tail bleeding to measure antibody titers.

7. *B. pertussis*-specific antibody measurements

Enzyme-linked immunosorbent assays (ELISAs) were performed using the Mouse anti-FHA IgG ELISA kit (Alpha Diagnostic International, 960-300-FMG), Mouse anti-PTX IgG ELISA kit (Alpha Diagnostic International, 960-130-PMG), and Mouse anti-PRN IgG ELISA kit (Alpha Diagnostic International, 960-230-PGG). Serum was diluted 1:250 in dilution solution, and 100 μl of diluted serum was added for 1 h at room temperature (RT). Plates were washed three times with PBS containing 0.1% Tween-20 (PBST), and 100 μl of mouse IgG-specific secondary antibody was added to each well. After 30 minutes of incubation at RT, plates were washed four times with PBST following the addition of 100 μl of TMB substrate reagent. The reaction was stopped after 5 min by adding 2 N sulfuric acid. Plates were then read at wavelengths of 450 nm and 630 nm.

8. Statistical analysis

Comparison between the two groups was evaluated using t-test, ordinary one-way ANOVA, and two-way ANOVA. In all tests, statistical significance was quantified as *P < 0.5, **P < 0.01, ***P < 0.001, and ****P < 0.0001. Statistical analysis was performed using the GraphPad Prism 9.5.0 program (Graph Pad Software, La Jolla, CA, USA).

II. RESULTS

Part 1.

1. Nasal immune profiling of *S. epidermidis*-inoculated mouse model under steady-state conditions

To examine the effects of *S. epidermidis* on the animal model, we intranasally inoculated *S. epidermidis* at 2×10^8 CFU for 5 consecutive days and isolated single immune cells after 1 day. Because of the low immune cell numbers in mouse nasal turbinate, we gathered nasal tissues from 5 mice in the control group. Nasal tissues of *S. epidermidis*-administered variants were collected from 2 mice due to highly increased live $CD45^+$ cells in response to bacterial stimulation, in line with augmented effector $CD4^+$ and $CD8^+$ T cells and diminished naïve $CD4^+$ and $CD8^+$ T cells (Figure 1B). Interestingly, the proportion and absolute cell numbers of RAR-related orphan receptor gamma t (RORγt) expressing $CD45^+$ cells were significantly upregulated compared with the control group, including T-box transcription factor TBX21 (T-bet) expressing $CD45^+$ cells (Figure 1C). We inspected the specific T cell populations in both control and *S. epidermidis*-inoculated mice. Except for the expression of T-bet^+ $CD4^+$ and $CD8^+$ T cells, RORγt^+ and GATA-binding protein 3 (GATA-3) expressing $CD4^+$ and $CD8^+$ T cells showed robust expansion (Figure 1D). To comprehensively observe different cell types compared to wild-type (WT) mice, we performed UMAP analysis and Phenograph clustering annotation (Figure 1E). Not only changes in T cell subsets but also major histocompatibility complex class-II^+ (MHC-II) neutrophils ($CD11b^+$ $Ly6G^+$ MHC-II^+) and conventional dendritic cells (cDCs, $CD11c^+$ MHC-II^+) were increased in post *S. epidermidis* association (Figure 1F). This finding indicated that functional antigen-presenting cells (APCs) were expanded, which present microbe antigens and induce $CD4^+$ T cell development. Furthermore, *S. epidermidis* promoted NK cell frequencies and cell numbers along with the number of regulatory T cells

(FOXP3$^+$ CD4$^+$) (Figure 1F). Taken together, our findings suggest that nasal commensals influence type 2 and type 17-related T cell responses and enhance MHC-II$^+$ expressing innate immune cells under steady-state conditions.

In addition, we observed the cytokine levels produced by immune cells following the gating strategy (Figure 2A). The proportions of IL-17a and tumor necrosis factor alpha (TNF-α) expressing CD45$^+$ cells were significantly increased, similar to the propensity of enhanced RORγt$^+$ and T-bet$^+$ populations (Figure 2B). Notably, local CD4$^+$ and CD8$^+$ T cells in *S. epidermidis*-administered mice highly expressed IL-17a$^+$ and TNF-α$^+$ (Figure 2C). However, γδ T cells exhibited a significant increase in the number of IL-17a$^+$ cells, whereas they showed an opposite decreased frequency (Figure 2D). Also, activated CD4$^+$ and CD8$^+$ T cells produced IL-17a$^+$ and TNF-α$^+$ simultaneously, suggesting its polyfunctional properties (Figure 2E). Consistent with the findings from the flow cytometry analysis, UMAP analysis revealed a substantial increase in CD4$^+$ and CD8$^+$ T cells expressing IL-17a$^+$ and TNF-α$^+$ (Figure 2F).

Taken together, *S. epidermidis*-evoked CD4$^+$ and CD8$^+$ T cells produced multiple cytokine profiles, particularly IL-17a$^+$ and TNF-α$^+$. These findings suggest that type 17 immune boosting occurred in a nasal commensal-dependent manner under homeostatic conditions. In addition, we implied that its mechanisms could be critical for bacterial clearance and that *S. epidermidis* may exert an antimicrobial response *in vivo*.

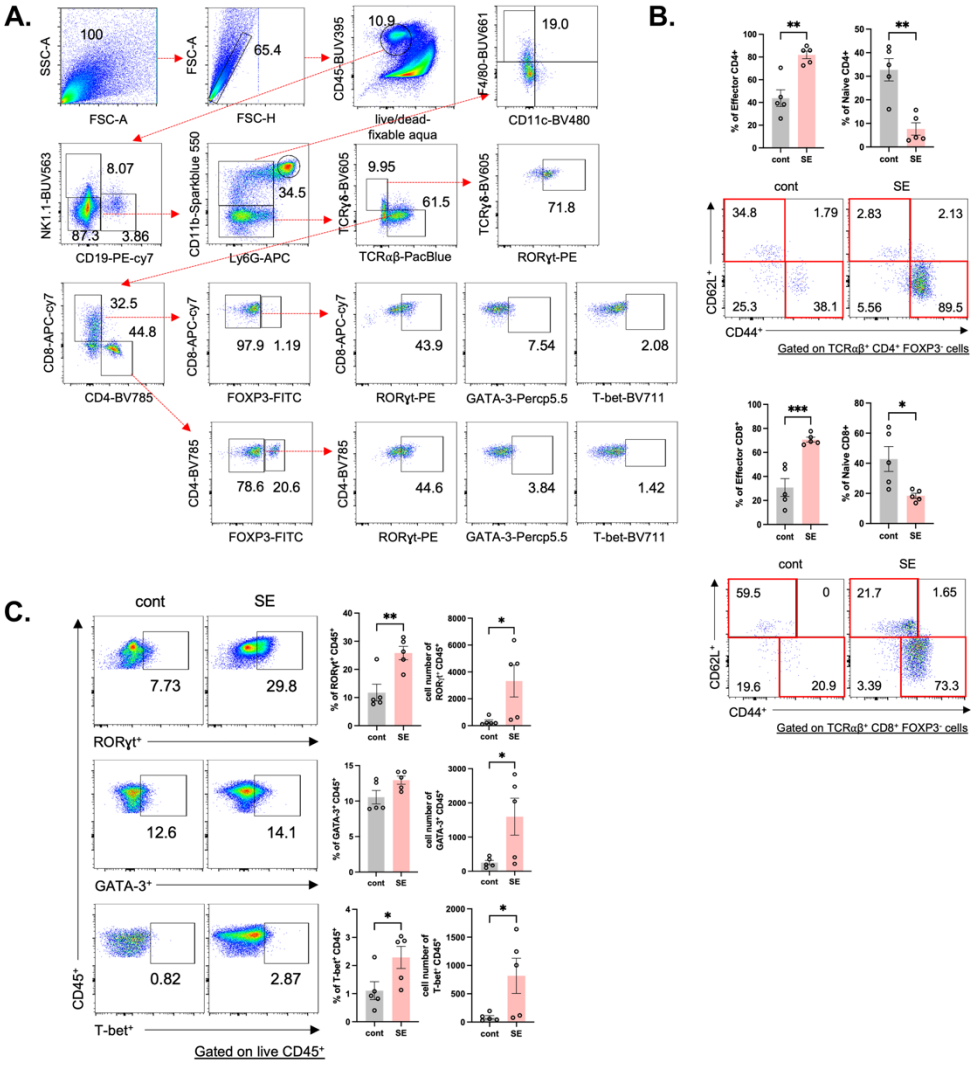

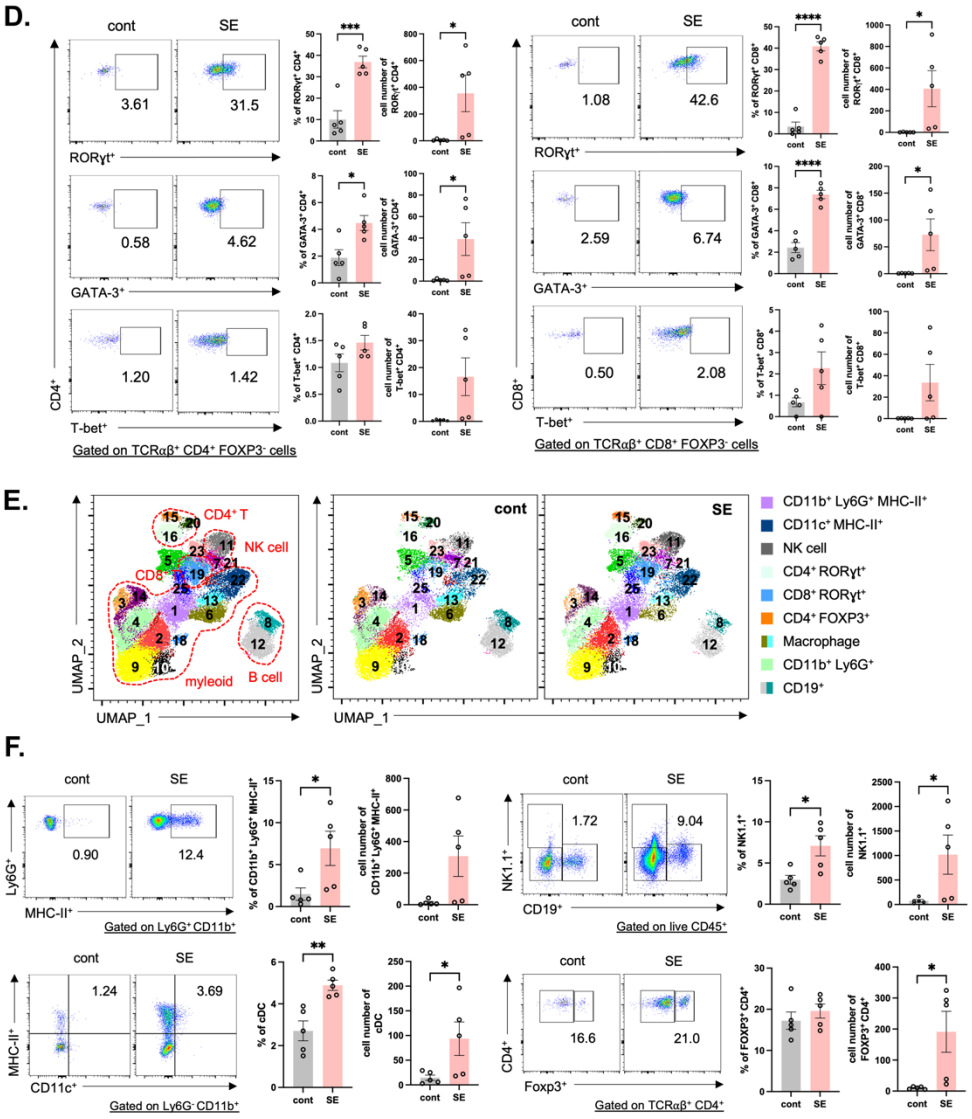

Figure 1. Kinetics of immune cell populations in the nasal cavity of *S. epidermidis*-administered mice (A) Gating strategy of the nasal immune cell population. **(B)** Quantification of frequencies and absolute cell numbers of effector and naïve $CD4^+$ and $CD8^+$ T cells. (n=5) **(C)** Quantification of frequencies and absolute cell numbers of $ROR\gamma t^+$, GATA-3^+, and T-bet^+ expressing live $CD45^+$ cells. (n=5) **(D)** Quantification of frequencies

and absolute cell numbers of RORγt^{+}, GATA-3^{+}, T-bet^{+} expressing CD4^{+} (left) and CD8^{+} (right) T cells were compared in control and *S. epidermidis*-administered groups. (n=5) **(E)** Increased and decreased cell types from all live CD45^{+} concatenated cells are presented in UMAP color-coded distinguished by Phenograph clustering. Each cluster number was annotated with cell markers. **(F)** Flow cytometry analysis of the increased populations shown in UMAP clustering. **(**cont: non-*S. epidermidis*-administered group, SE: *S. epidermidis*-administered group)

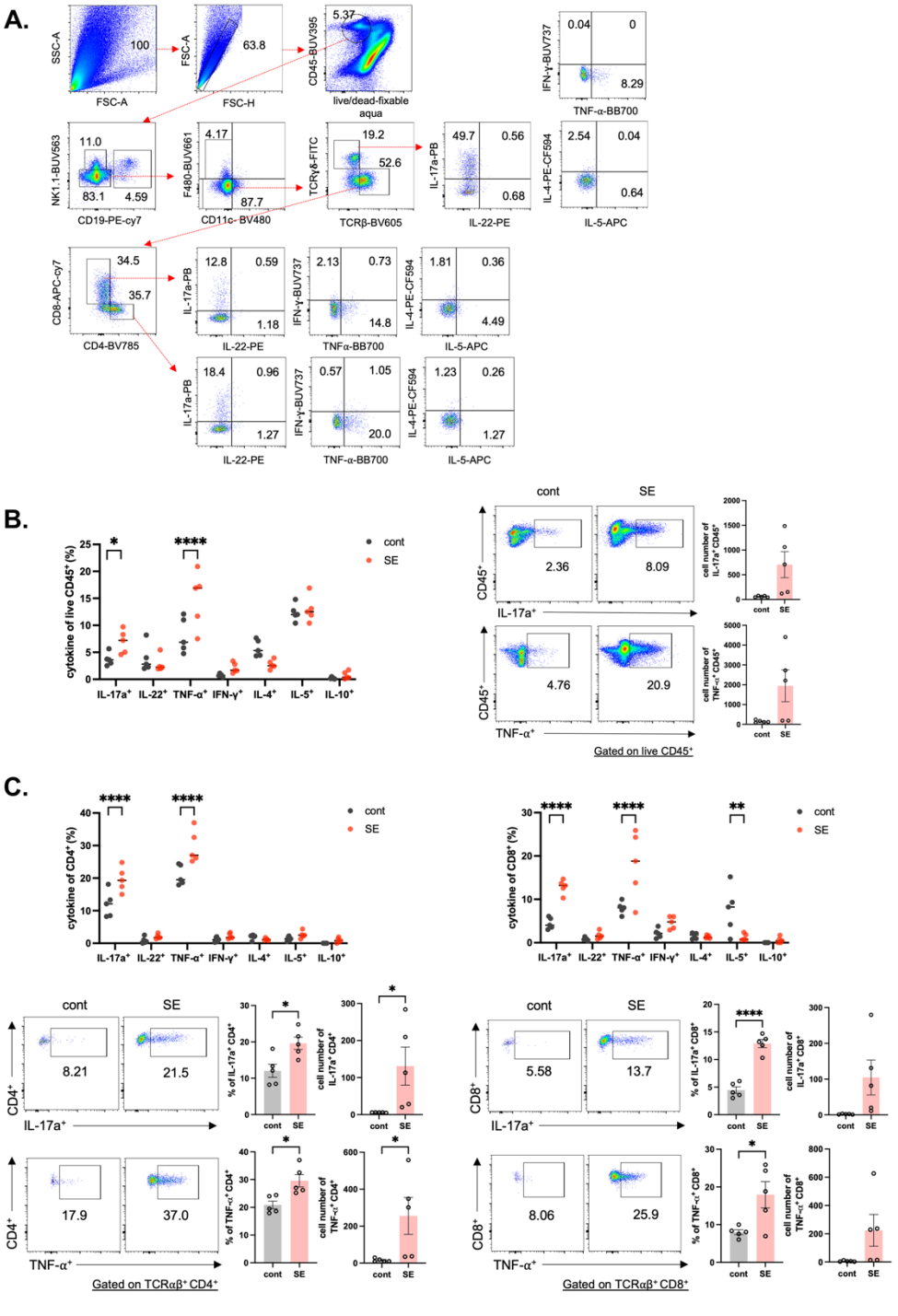

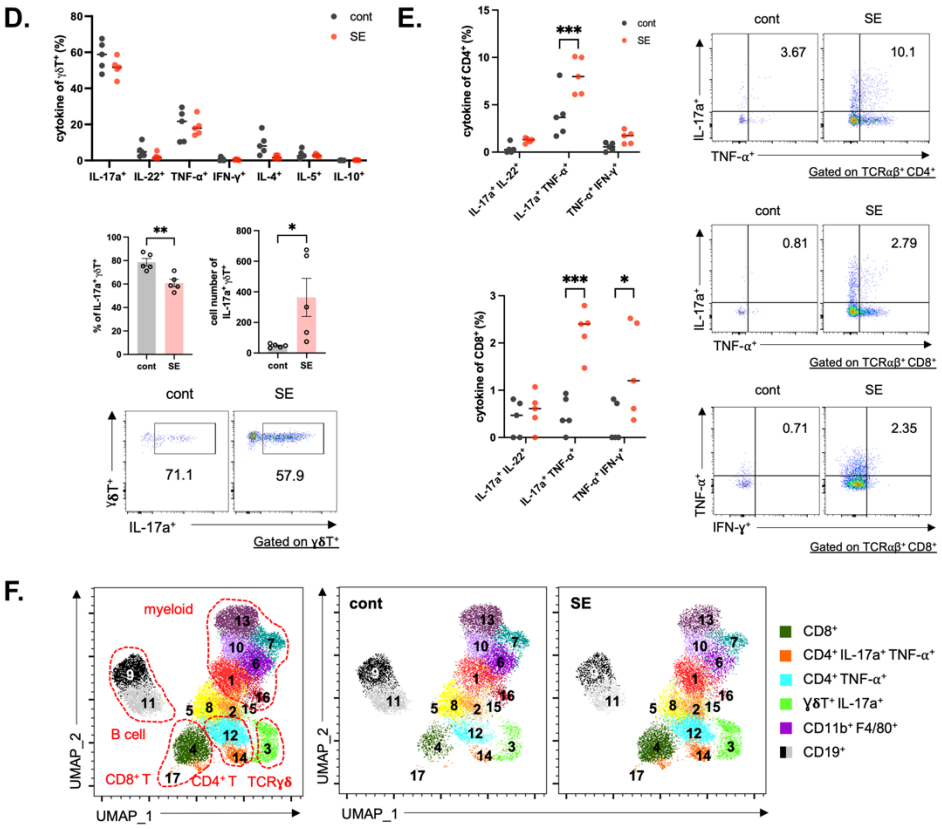

Figure 2. Kinetics of immune cell cytokines in the nasal cavity of *S. epidermidis*-administered mice (A) Gating strategy of nasal immune cell cytokines. **(B)** Quantification of frequencies and cell numbers of multiple cytokines from live CD45$^+$. (n=5) **(C)** Quantification of frequencies and cell numbers of IL-17a$^+$ and TNF-α$^+$ expressing CD4$^+$ and CD8$^+$ T cells. (n=5) **(D)** Quantification of frequencies and cell numbers of IL-17a$^+$ expressing γδ T cells. (n=5) **(E)** Quantification of frequencies of stimulated CD4$^+$ and CD8$^+$ T cells producing each combination of IL-22$^+$, IL-17a$^+$, TNF-α$^+$, and IFN-γ$^+$ cytokines were compared in control and *S. epidermidis*-administered group. (n=5) **(F)** Increased and decreased cell types from all live CD45$^+$ concatenated cells are presented in UMAP color-coded distinguished by Phenograph clustering. Each cluster number was annotated with cell markers. (cont: non-S. *epidermidis*-administered group, SE: *S. epidermidis*-administered group)

2. *S. epidermidis*-mediated defense against *B. pertussis* infection mouse model

To validate the protective properties of *S. epidermidis* against *B. pertussis* infection *in vivo*, we primarily intranasally challenged mice with *B. pertussis* at 8×10^8 CFU. We evaluated the pathogenesis in mice at 3-, 5-, 7-, and 14-days post-infection (dpi) using lung bacterial titers and morphologies of infected lung tissues. Bacterial colony numbers on BGA plates were counted and CFUs were determined. A similar level of CFU was measured at 3,5,7 dpi, except for 14 dpi, which showed a great reduction in the bacterial load (Figure 3B). In addition, the histological analysis of the 3,5,7 dpi mouse lung indicated increased inflammation compared to 14 dpi and control mouse lung, showing the convalescence stage starting at day 14 (Figure 3C). We also performed histopathological analysis by scoring H&E-stained sections representing alveolitis and bronchiolitis, indicating infiltration of inflammatory cells (Figure 3D). Similar to the results observed in bacterial burden, histology scoring also revealed a significantly reduced inflammation phenotype at 14 dpi compared to the groups at 3, 5, and 7 dpi.

After confirming *B. pertussis* infection with a bacterial burden of 8×10^8 CFU, we investigated whether intranasal pretreatment with *S. epidermidis* suppressed *B. pertussis* infection. We colonized *S. epidermidis* for five consecutive days at 2×10^8 CFU prior to *B. pertussis* infection and inspected lung pathogenesis at 3 dpi (Figure 4A). Compared to *S. epidermidis* non-administered mice, the transcript level of *B. pertussis* was lower, suggesting that nasal commensals suppressed *B. pertussis* invasion (Figure 4B). Also, the bacterial load in mice lungs was diminished compared with that in the control group (Figure 4C). In addition, we performed H&E staining to examine the inflammatory status of the lung tissue (Figure 4D). Although both infected mice showed an increased abundance of cellular infiltration compared to the non-infected mice, we observed lower immune cell infiltration in the *S. epidermidis*-pretreated group than in the non-inoculated group. Lung histopathology scores in alveolitis and bronchiolitis were both lower as commensals were

colonized before pathogen infection, suggesting lessened pulmonary inflammation. Taken together, these results indicate that nasal commensals can prevent acute respiratory pathogen infection.

To assess whether different immune phenotypes occurred in response to *S. epidermidis*-dependent manner, we conducted immune profiling in lung and nasal samples from *B. pertussis*-infected mice. Between days 3 and 5 dpi in *B. pertussis*-infected mice, innate immune cells such as neutrophils, macrophages, and DCs are activated in the lungs[5]. Consistent with existing studies, our data revealed a significant increase in these cell types in mice infected with *B. pertussis*. Unexpectedly, however, when *S. epidermidis* was administered as a prior treatment, we observed a reduction in DCs and $Ly6C^-$ macrophage populations, whereas $Ly6C^+$ macrophages increased compared with mice untreated with *S. epidermidis* (Figure 5A). Regulatory T cells also exhibited a robust increase in mice infected only with *B. pertussis*, but a decrease was observed when *S. epidermidis* was colonized (Figure 5B). This suggests that regulatory T cells, which play a role in maintaining immune homeostasis, may exert a mitigating effect on respiratory pathogen infection when *S. epidermidis* is present, resulting in a milder immune response. Under steady-state conditions, as *S. epidermidis* increased the expression of RORγt in T cells, we observed the proportions of $ROR\gamma t^+$ $CD4^+$, $CD8^+$, and γδ T cells. However, within the lung, we did not observe a significant increase in these cell populations. Additionally, cytokine analysis confirmed a notable increase in IL-17a-secreting γδ T cells and TNF-α-secreting $CD4^+$ and $CD8^+$ T cells.

Given that *B. pertussis* infection on the nasal mucosal surface spreads to the LRT, activation of local immune responses may exert a crucial impact on the reduction of bacteria. Interestingly, unlike the lung tissue, there were no significant changes in the population of innate immune cells except for a reduction in $Ly6C^-$ macrophages (Figure 6A). Consistent with the lung, the population of regulatory T cells showed a further

decrease in the presence of *S. epidermidis* (Figure 6B). Upon investigating whether *S. epidermidis* is involved in the modulation of adaptive immune cells, the overall $CD4^+$, $CD8^+$, and γδ T cells exhibited a significant augmentation compared to the group infected with *B. pertussis* (Figure 6C). Furthermore, $CD4^+$ T cells and γδ T cells expressing RORγt also exhibited a substantial increase, followed by the expansion of proinflammatory secreting $CD4^+$, $CD8^+$, and γδ T (Figure 6D, E). In summary, our findings demonstrated that type 17 immune cells were boosted by *S. epidermidis* before *B. pertussis* infection, contributing to the suppression of respiratory pathogen infection. In particular, primary inhibition of *B. pertussis* invasion in the nasal turbinate led to more effective prevention of bacterial infection in the lungs.

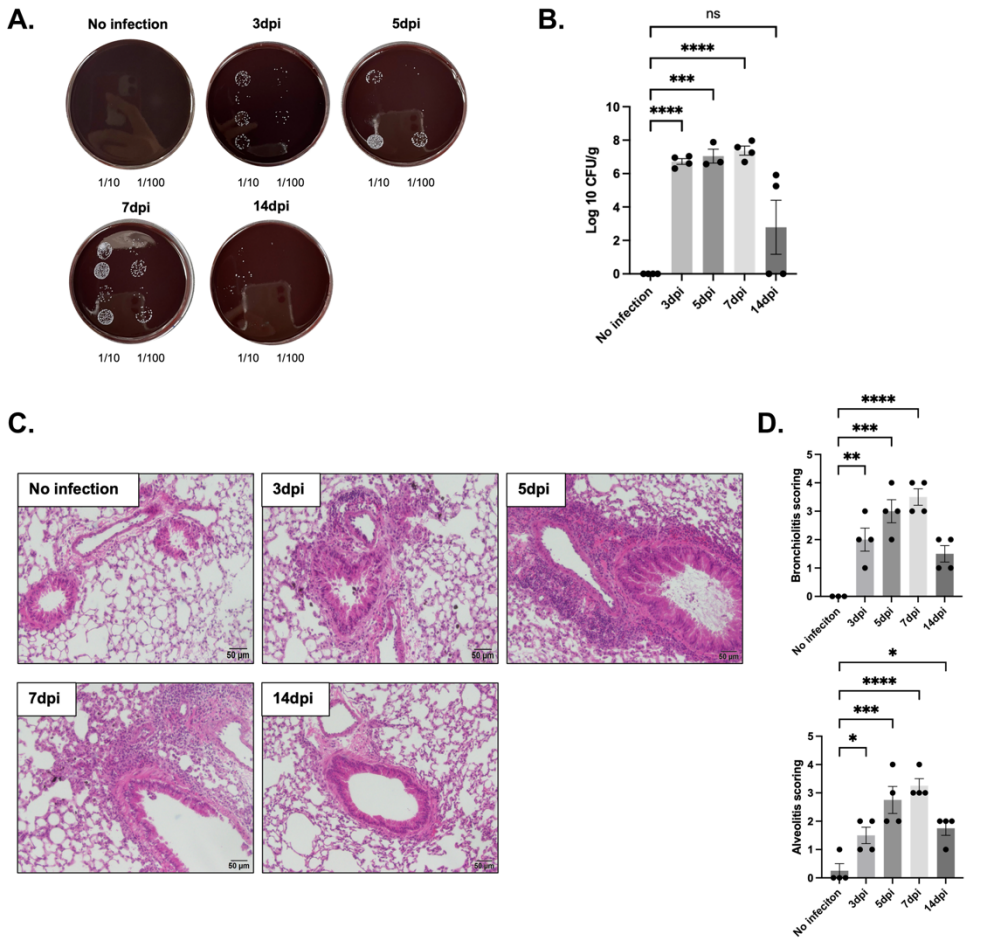

Figure 3. Pathogenesis of the *B. pertussis*-infected mouse model dependent on the time point (A,B) Bacterial titer was determined in the mouse lung following *B. pertussis* infection at the indicated time point. Plate images of bacterial cultures plated at serial dilutions from 1:10 to 1:100. Colony numbers were counted and calculated as log10 of CFU/lung tissue weight (g). (n=4) **(C)** Histological analysis of the infected mouse lung tissue sections. Scale bars, 50 μm. **(D)** H&E-stained sections were examined by a single blinded observer using a 0-4 scale (0, no inflammation; 1, mild inflammation; 2, moderate inflammation; 3, marked inflammation; 4, severe inflammation) for bronchiolitis and alveolitis, as previously described[27].

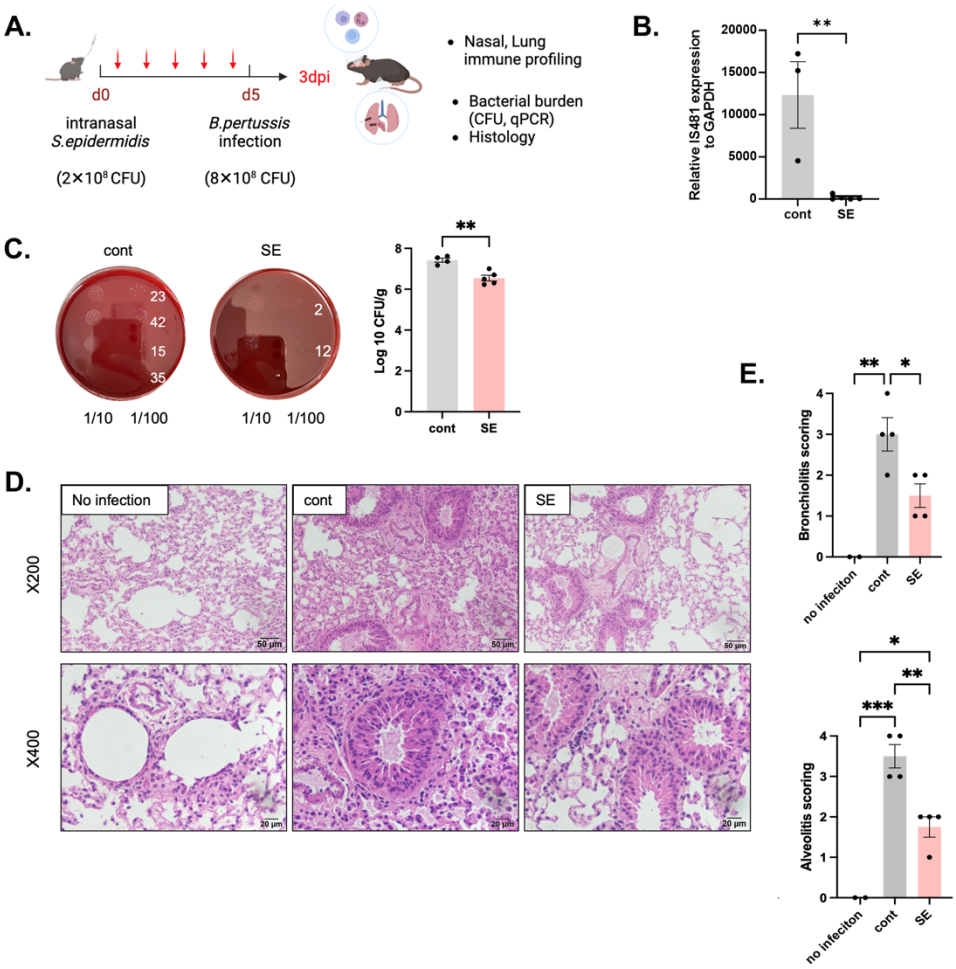

Figure 4. Intranasal *S. epidermidis* colonization drives suppression of *B. pertussis* infection (A) Experimental scheme of this study. Mouse were intranasally inoculated with *S. epidermidis* for 5 consecutive days at 2×10^8 CFU before *B. pertussis* infection. **(B)** Relative mRNA expression levels of *B. pertussis* (IS481) as determined by quantitative real-time PCR. Changes in the mRNA levels were normalized to *GAPDH,* and fold-changes were calculated and compared with the corresponding uninfected mouse lung tissues (n=5). **(C)** Plate images of bacterial cultures plated at dilutions from 1:10 to 1:100. Colony numbers were counted and calculated as log10 of CFU/lung tissue weight (g) (n=5). **(D)**

H&E staining of lung tissues in *B. pertussis*-infected or control mice. Scale bars, 50 μm. **(E)** H&E-stained sections were examined by a single blinded observer using a 0-4 scale (0, no inflammation; 1, mild inflammation; 2, moderate inflammation; 3, marked inflammation; 4, severe inflammation) for bronchiolitis and alveolitis, as previously described[27]. (cont : non-*S. epidermidis*-administered group, SE: *S. epidermidis*-administered group)

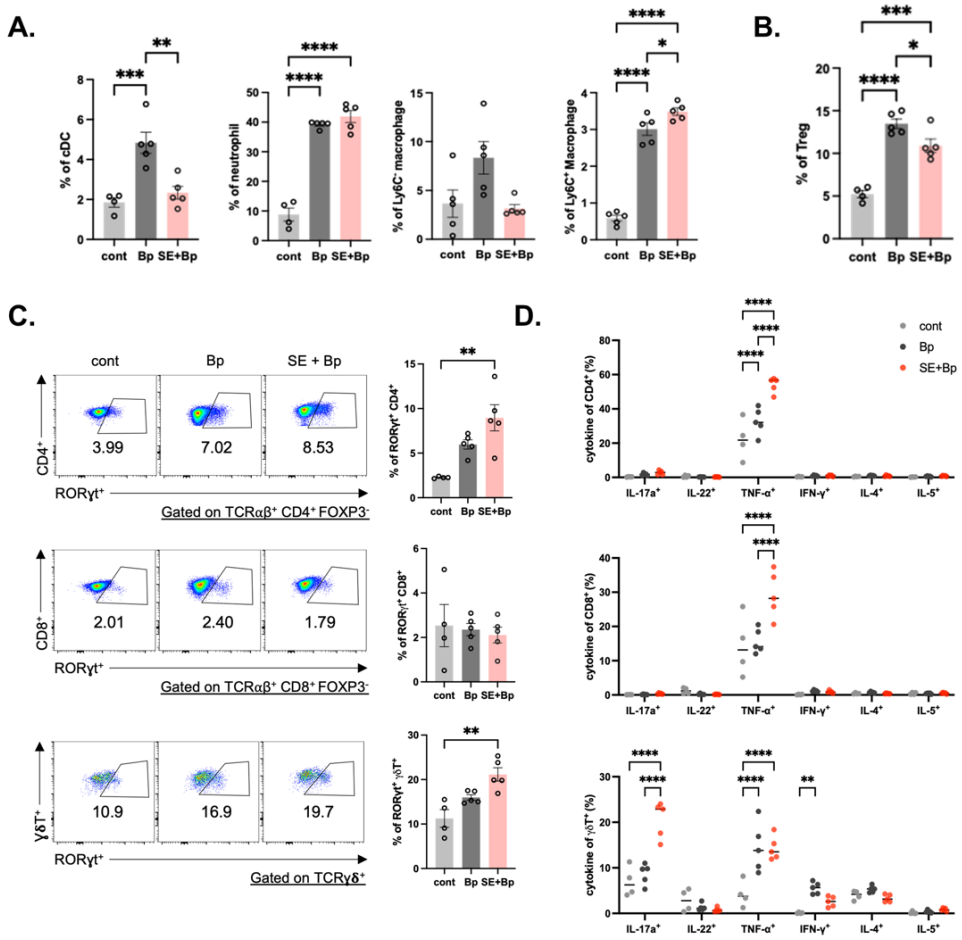

Figure 5. Major phenotypic alterations within pulmonary immune responses following *S. epidermidis* colonization and *B. pertussis* infection (A) Quantification of the percentage of cDC, neutrophil, Ly6C$^-$ macrophage, and Ly6C$^+$ macrophage populations. (n=5) **(B)** Quantification of the percentage of regulatory T cells among total CD4$^+$ T cells. (n=5) **(C)** Quantification percentage of RORγt$^+$ expressing CD4$^+$, CD8$^+$, and γδ T cells. (n=5) **(D)** Quantification percentage of cytokine levels produced by CD4$^+$, CD8$^+$, and γδ T cells. (n=5) (cont : non-infection group, Bp: only *B. pertussis*-infected group, SE+Bp : prior *S. epidermidis* administration with *B. pertussis*-infected group)

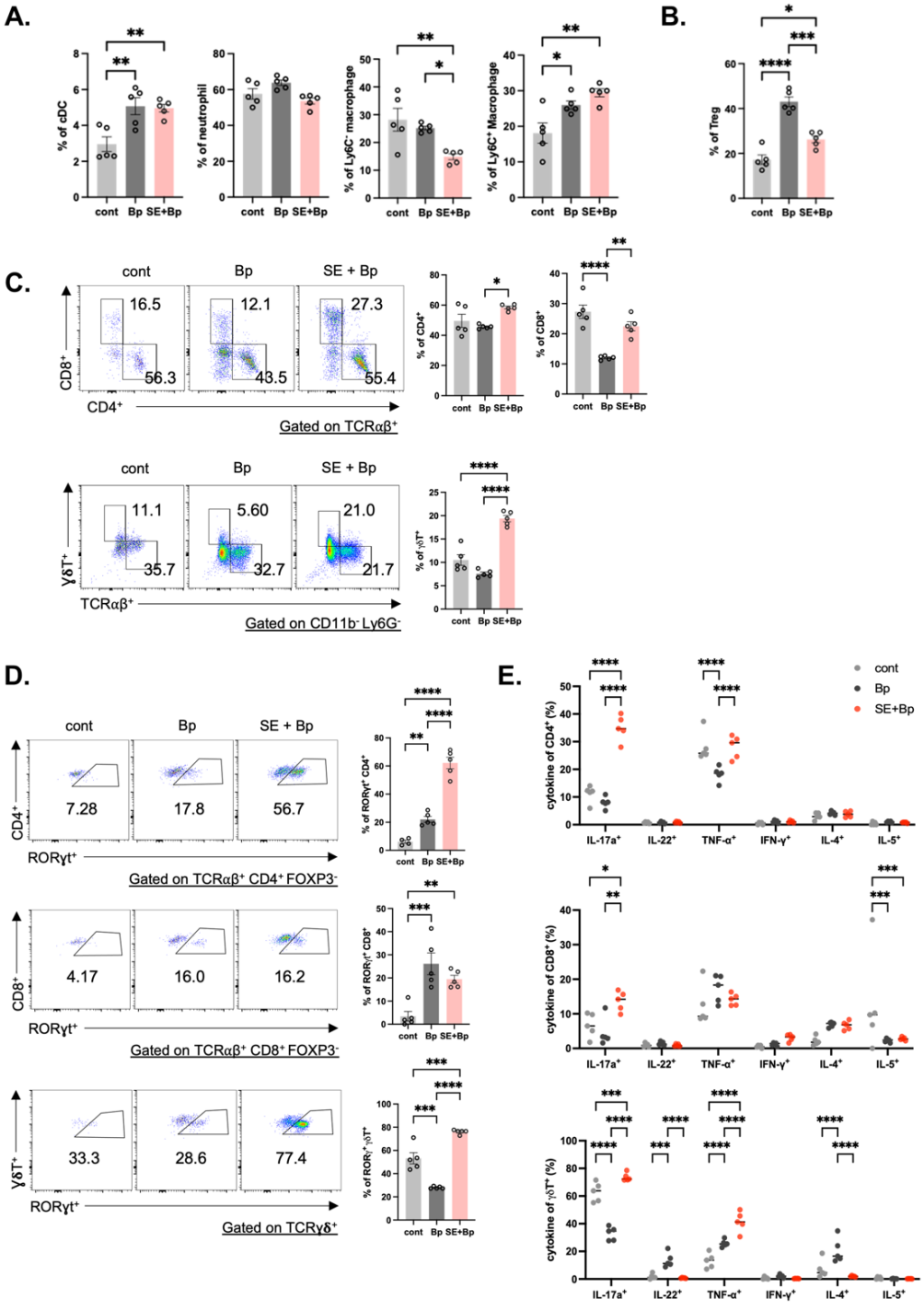

Figure 6. Major phenotypic alterations within nasal immune responses following *S. epidermidis* colonization and *B. pertussis* infection (A) Quantification of the percentage of cDC, neutrophil, Ly6C^{-} macrophage, and Ly6C^{+} macrophage populations. (n=5) **(B)** Quantification of the percentage of regulatory T cells among total CD4^{+} T cells. (n=5) **(C)** Quantification percentage of overall CD4^{+}, CD8^{+}, and γδ T cells. (n=5) **(D)** Quantification percentage of RORγt^{+} expressing CD4^{+}, CD8^{+}, and γδ T cells. (n=5) **(E)** Quantification percentage of cytokine levels produced by CD4^{+}, CD8^{+}, and γδ T cells. (n=5) (cont : non infection group, Bp: only *B. pertussis*-infected group, SE+Bp : prior *S. epidermidis* administration with *B. pertussis*-infected group)

Part 2.

1. Development of an NRaP vaccine

To overcome the limitations of the current aP vaccine, we developed recombinant pertussis antigen proteins that were transformed in *Escherichia coli (E. coli)* to increase immunogenicity, establish long-term immune efficacy, and reduce side effects. Although PTX of the current aP vaccine has low immunogenic properties because of chemical detoxification, we mitigated PTX toxicity by using R9K/E129G mutations to overcome the limitations of conventional vaccines. We also removed the C-terminal translocation domain and N-terminal signal sequence from the PTX and PRN antigens. These were eliminated to introduce quick and accurate immunogenic responses. Three types of PTX, FHA, and PRN genes were cloned into the pGE-ChaH2 vector and transformed into *E. coli* competent cells (Figure 1A). When external proteins are transformed into *E. coli,* it is difficult to produce catalytically active protein due to protein misfolding and insolubility, which leads to low protein yields. To overcome these problems, ChaH2, a novel RNA chaperone technique, was used and incorporated as a fusion partner. ChaH2 binds with RNA and aids in the folding of large protein complexes, enabling massive production with high efficiency (Figure 1B). Strains BL21 Star™(DE3)pLysS and SHuffle®T7 have optimal growth temperatures of 37°C and 30°C, respectively. Lowering the temperature during protein overexpression is a strategy to enhance protein solubility and activity, ensuring the slow and proper formation of proteins. In LB broth culture, ChaH2-FhaB and ChaH2-Prn were grown at 37°C, while ChaH2-PtxA^{m} was cultured at 30°C until reaching an OD600nm of approximately 0.7. The temperature was then reduced to 20°C, and 1 mM of IPTG was added to induce genetic expression, followed by 16-20 h of cultivation. Harvested cells were centrifuged at 4,000 rpm for 20 min at 4°C to obtain cell pellets. *E. coli* cultures were grown with and without IPTG, followed by centrifugation to obtain cell pellets. The lysate obtained through sonication is represented as the total lysate (T). Subsequently,

centrifugation yielded the supernatant, known as the soluble fraction (S), while the remaining pellet was resuspended and combined with sodium dodecyl sulfate (SDS) loading buffer (P), resulting in a combination of the soluble fraction and suspended pallet representing the total lysate, denoted as T. To assess the expression levels and solubility, we performed sodium dodecyl sulfate–polyacrylamide gel electrophoresis (SDS-PAGE) (Figure 1C). The molecular weights of ChaH2-PtxA^{m}, ChaH2-FhaB, and ChaH2-Prn were approximately 52 kDa, 75 kDa, and 85 kDa, respectively. The presence of protein bands at these sizes, indicated by red arrows and compared with the protein marker (M), confirmed the remarkable expression of the proteins. Various bands in the background are *E. coli*-derived proteins. The harvested cells were resuspended in lysis buffer (50 mM Tris-Cl, pH 7.5, 300 mM NaCl, 10% Glycerol) and sonicated for cell disruption. The resulting cell lysate was centrifuged at 13,000 RPM for 15 minutes at 4°C to obtain the supernatant. After filtering with a 0.45 μm filter, Ni^{2+} affinity chromatography was conducted (Figure 1D). The sample was loaded onto a nickel column, and buffer (50 mM Tris-Cl, pH 7.5, 300 mM NaCl, 1% Triton X-114) added to remove bacterial endotoxins. Triton X-114 (1%) was added to the antigen protein, and the mixture was incubated at 4°C with rotation for a minimum of 1 h. After transfer to a 37°C water bath for 20 minutes of incubation, the solution is centrifuged at 20,000 RCF for 10 minutes at 25°C to harvest the upper phase. Elution of the recombinant antigen was achieved by applying a linear gradient of imidazole concentration using buffer (50 mM Tris-Cl, pH 7.5, 300 mM NaCl, 10% Glycerol, 10 mM Imidazole, 2 mM β-mercaptoethanol, 0.1% Tween-20) and buffer (50 mM Tris-Cl, pH 7.5, 300 mM NaCl, 10% Glycerol, 1 M Imidazole for FhaB & PTxA^{m} / 1.5 M Imidazole for Prn, 2 mM β-mercaptoethanol, 0.1% Tween-20). The filtered supernatant (T), protein marker (M), and purified fractions were subjected to SDS-PAGE analysis to confirm the presence of the recombinant antigen. After endotoxin removal, the antigen proteins were concentrated using a centrifugal filter. Quantification is performed by SDS-PAGE analysis using BSA as a standard. Band intensities are compared with BSA, and for ChaH2-FhaB, approximately 3 μL corresponds to 4 μg, for ChaH2-PtxA^{m}, 4 μL corresponds to 4 μg, and

for ChaH2-Prn, 4 μL corresponds to 4 μg. The concentrations were determined to be ChaH2-FhaB 1.33 μg/μL, ChaH2-PtxA^{m} 1 μg/μL, and ChaH2-Prn 1 μg/μL (Figure 1E). Endotoxin measurement was performed using the Pierce™ Chromogenic Endotoxin Quant Kit. If endotoxin levels were high, an additional removal step was performed, and if the concentration was low, further concentration was carried out. Endotoxin measurements were repeated as necessary.

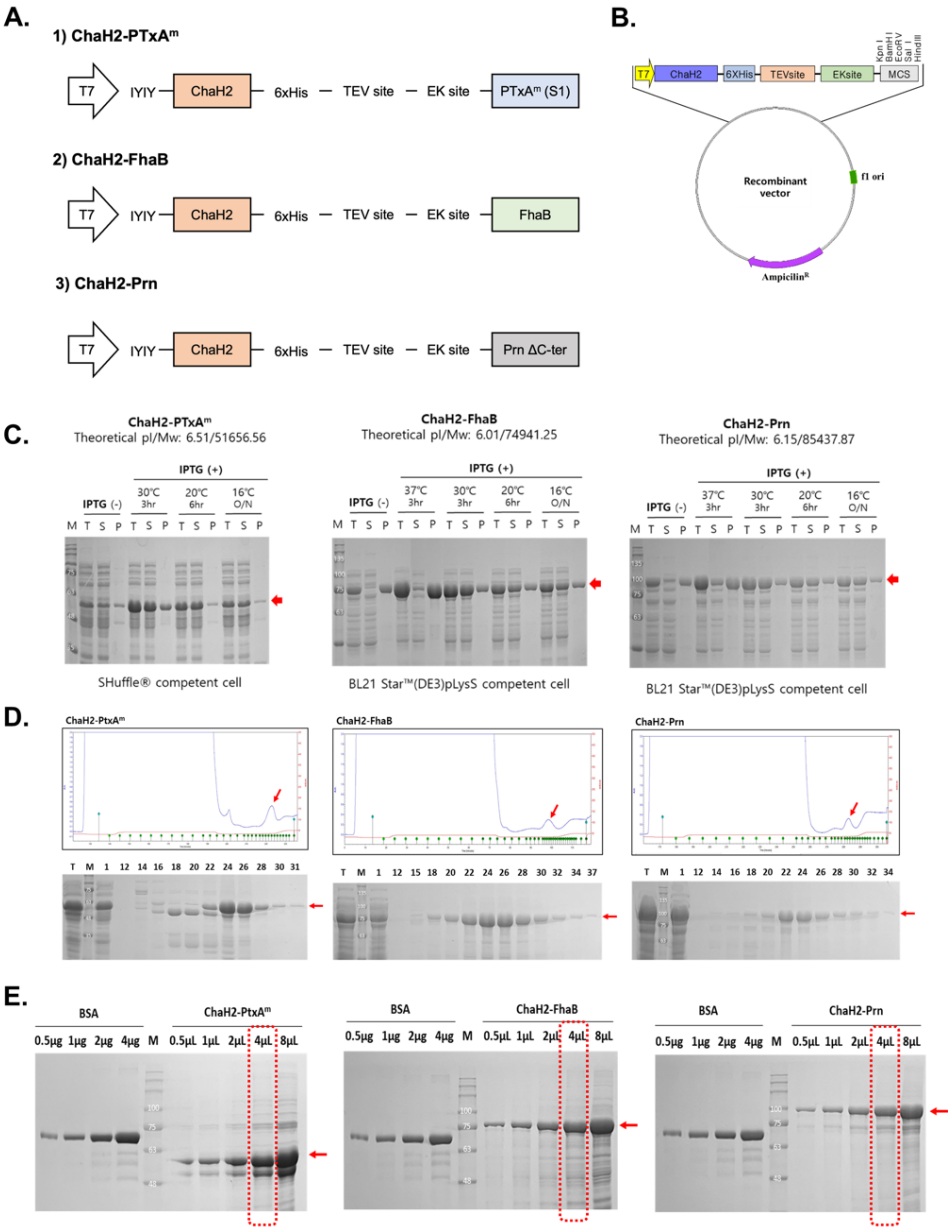

Figure 1. Characterization of NRaP vaccines (A) The construct of vaccine antigens. **(B)** ChaH2 expressing vector map. The three pertussis virulence factors were cloned into its vector and transformed with *E. coli*. "M" represents a broad protein marker, "T" denotes the total lysate, "S" indicates the soluble fraction, and "P" refers to the insoluble fraction

(pellet). **(C)** The solubility test of ChaH2-PtxAm^{m} (left), ChaH2-FhaB (middle), and ChaH2-Prn (right) recombinant proteins was performed using SDS-PAGE analysis. **(D)** SDS-PAGE analysis after performing Ni^{2+} affinity chromatography. The results represented ChaH2-PtxAm^{m} (left), ChaH2-FhaB (middle), and ChaH2-Prn (right). **(E)** The protein concentrations were measured by SDS-PAGE analysis using BSA as a standard. The results represented ChaH2-PtxAm^{m} (left), ChaH2-FhaB (middle), and ChaH2-Prn (right).

2. Analyzing the immunogenicity profiles of the NRaP vaccine

To assess the protective effects of NRaP vaccines, we vaccinated intramuscularly 2 times at 2-week intervals with 1/10 human dose of Infanrix and the NRaP vaccine (Figure 2A). The immunogenicity of the NRaP vaccine was evaluated by analyzing both systemic neutralizing antibodies and cellular immune responses. Serum samples were collected at 2 weeks after the 1st and 2nd immunization. First, we assessed the pertussis antigen-specific antibody titers compared with those of PBS and the existing aP vaccine, Infanrix (Figure 2B). Unfortunately, the levels of PTX-specific IgG were observed to be lower than Infanrix, whereas FHA-specific IgG levels were comparable. In contrast, PRN-specific IgG levels were significantly higher than Infanrix-immunized individuals. To determine the preventive effects against *B. pertussis* from the respiratory tract following immunization, we challenged with *B. pertussis* post 2 weeks of 2nd immunization. Unchallenged mice were used as controls. At 3 dpi, lung homogenates were incubated on BGA plates and CFU counts were counted. All mice immunized with pertussis antigens showed a substantial reduction in bacterial titer compared to mice immunized with PBS (Figure 2C). We also observed the bacterial burden by measuring transcription levels in the mouse lung (Figure 2D). In a single mouse administered Infanrix, the relative abundance of murine lung bacterial mRNA expression was comparable that in mice subjected to PBS immunization. Conversely, NRaP-immunized mice exhibited a significant reduction in mRNA levels compared to the vehicle group. Through a comparison of CFU and IS481 mRNA levels to assess the bacterial burden, immunization with NRaP exhibited complete immunity against *B. pertussis*, indicating enhanced vaccine immunogenicity.

Given that *S. epidermidis* colonization affects nasal immune modulation and is effective in suppressing *B. pertussis*, we aimed to investigate whether a combination strategy of vaccine and nasal commensal ultimately enhances vaccine immunogenicity. Therefore, we intranasally administered *S. epidermidis* for 5 consecutive days at 2×10^8 CFU before twice

intramuscular immunization. Serum samples were obtained 14 days after 2nd immunization (Figure 3A). Contrary to our expectations, the group treated with *S. epidermidis* exhibited lower levels of antigen-specific IgG than those observed with the conventional vaccine alone (Figure 3B).

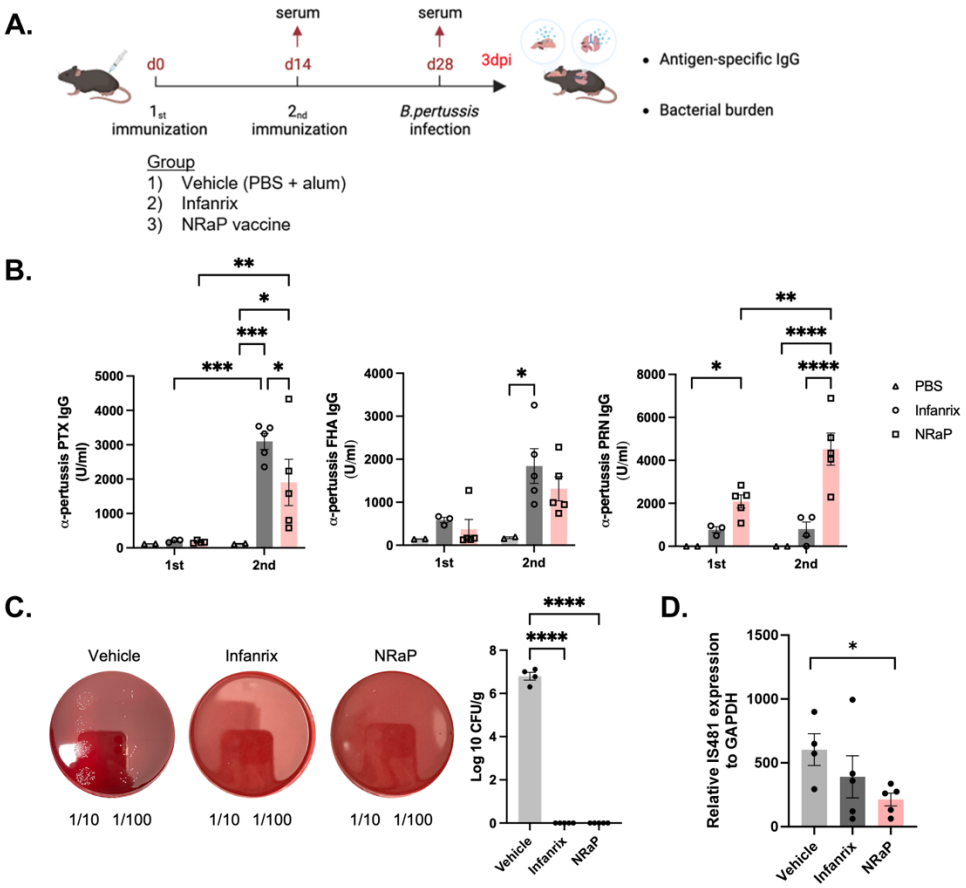

Figure 2. Investigating the immunogenicity of the NRaP vaccine in *B. pertussis*-infected mouse model. (A) Experimental scheme of this study. Cohorts of C57BL/6 mice were vaccinated twice with Vehicle, Infanrix, and NRaP vaccines. The vehicle and subunit vaccine were mixed with alum hydroxide at an equivalent volume of the immunogens. Infanrix and the recombinant proteins contained equal amounts of PTX (5 μg), FHA (5 μg), and PRN (1.6 μg). Mice were vaccinated intramuscularly twice at 2-week intervals, following *B. pertussis* infection at 8×10^{8} CFU/40 μl. Mice were sacrificed at 3 dpi. **(B)** *B. pertussis* antigen-specific IgG levels from each vaccinated mouse. Serum samples were collected at day 14, 28 post-vaccinations, and they were labeled as 1st and 2nd, respectively.

(n=4/Vehicle group, n=5/Infanrix, NRaP group) **(C)** Plate images of bacterial cultures plated at dilutions from 1:10 to 1:100. Colony numbers were counted and calculated as log10 of CFU/lung tissue weight (g). (n=4/Vehicle, n=5/Infanrix, NRaP) **(D)** Quantitative mRNA expression of *IS481* genes in Vehicle, Infanrix, or NRaP-immunized mouse lung tissues at 3 dpi of the *B. pertussis*-challenged model. The changes in the mRNA levels were normalized to *GAPDH,* and the fold-changes were calculated in comparison to corresponding uninfected mice lung tissues. (n=4/Vehicle, n=5/Infanrix, NRaP)

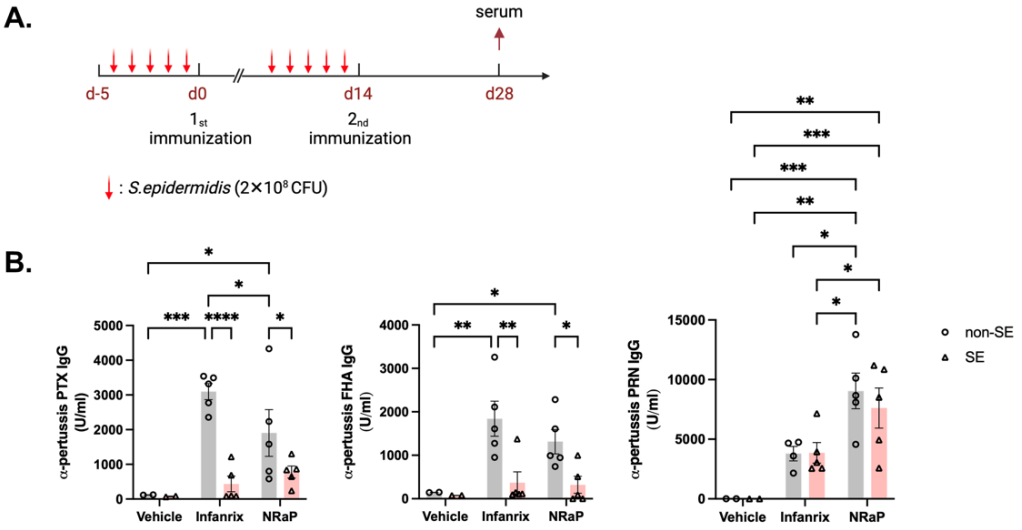

Figure 3. Evaluating vaccine immunogenicity through a dual strategy of nasal commensal and immunization (A) Experimental scheme of this study. Cohorts of C57BL/6 mice were vaccinated twice with PBS, Infanrix, and NRaP vaccines. PBS and the subunit vaccine were mixed with alum hydroxide at an equivalent volume of the immunogens. Infanrix and the recombinant proteins contained equal amounts of PTX (5 μg), FHA (5 μg), and PRN (1.6 μg). Mice were vaccinated intramuscularly twice at 2-week intervals. Before the two immunizations, nasal inoculation of *S. epidermidis* was performed with 2×10^8 CFU. Serum was collected at day 28 post-vaccination. **(B)** *B. pertussis*-antigen-specific IgG levels from each vaccinated mouse. (n=2/Vehicle, n=4/Infanrix, n=5/NRaP) (non-SE : non-*S. epidermidis*-administered group, SE : prior *S. epidermidis* administration group)

III. DISCUSSION

Our study revealed that *S. epidermidis* has immunomodulatory functions and antibacterial properties against *B. pertussis* infection. We selected 50 strains of *S. epidermidis* from the nasal flora of patients with chronic rhinosinusitis and healthy individuals and conducted a study using the 13th isolate (SE#13). Screening involved co-culturing DCs primed with microbial antigens from *S. epidermidis* and naive CD8$^+$ T cells. Among the 50 isolates, SE#13-primed DCs uniquely induced the differentiation of CD8$^+$ T cells, leading to IFN-γ secretion, without inducing Treg cells. Consequently, SE#13 was chosen for further investigation, and we refer to it as *S. epidermidis*.

In part 1, we analyzed nasal immune cells from *S. epidermidis*-inoculated and WT mice. Following intranasal *S. epidermidis* administration, there was a significant increase in NK cells and conventional DCs and a decrease in B cells and macrophages. Furthermore, the expression of MHC-II molecules, which play a role in antigen presentation to CD4$^+$ T cells, increased after *S. epidermidis* colonization. Subsequent analysis revealed that among various APC subsets, the cell types exhibiting the highest increase in MHC-II$^+$ expression were neutrophils and DCs. Neutrophils contribute the activation of T cell responses by secreting chemokines that attract T cells to the site of inflammation. They can also deliver antigens to DCs, enhancing their effectiveness as initiators of naive CD4$^+$ T cell activation[28]. Therefore, our results indicated that microbial components activated neutrophils and DCs with APC-like characteristics. This, in turn, affected on the stimulation and differentiation of CD4$^+$ T cells. We also observed adaptive immune responses and identified a robust increase in RORγt$^+$ immune cells, particularly CD4$^+$ and CD8$^+$ T cells. As well as the Th17-type transcription factor, the proportion of IL-17a-expressing CD4$^+$ and CD8$^+$ T cells was significantly upregulated compared with WT mice. We also revealed an enhanced level of GATA-3$^+$ expression in T cells, but no differences in IL-4$^+$ and IL-5$^+$ expression, indicating that these cells are non-functional. Comprehensively, this research suggests that nasal commensals mediate innate and adaptive immunity under steady-state conditions. Our data

also implied that *S. epidermidis* colonization in the nasal cavity boosts type 17 T cells, which reinforces barrier function and immunity with antimicrobial defense. Although the role of *S. epidermidis* as a skin commensal has been extensively elucidated, its function as a nasal commensal is poorly understood. Previous studies that investigated the impact of *S. epidermidis* on the host nasal immune system have focused mostly on innate immune responses and antiviral responses. One study indicated that *S. epidermidis* stimulates the nasal epithelium and subsequently produces antimicrobial peptides that contribute to pathogen exclusion[22]. According to another study, *S. epidermidis* activated IFN-λ expression by stimulating the respiratory epithelium, resulting in suppression against influenza virus[23]. Given the current increasing incidence of respiratory tract infections, our results provide new evidence that the antimicrobial defensive role of nasal commensal microorganisms plays a significant role in the future development of treatments. Our study has not elucidated the specific causation of the increased population of IL-17-expressing cells; therefore, further investigation is needed. A growing body of research has explored multiple instances of IL-17 induction in various tissues by microbe antigens. One study elucidated the role of IL-17 in the development of pulmonary fibrosis, highlighting that IL-17 primarily produced by lung microbiota serves as a key driver[29]. In addition, the mechanisms of the IL-17 response involve the Toll-like receptor (TLR)-Myeloid differentiation primary response 88 (MyD88) signaling pathway from alveolar macrophages. Furthermore, the functional mechanisms of the IL-17 response induced by *S. epidermidis* as a commensal microbe residing on the skin were investigated. It has been observed that IL-17 secretion by T cells is diminished in the absence of MyD88 and the IL-1 receptor[30]. According to another study, *S. epidermidis* predominantly induces IL-17a production by $CD8^+$ T cells, with a mechanism involving $CD103^+$ DCs and $CD11b^+$ DCs[24]. Considering studies on type 17 immune responses induced by microbe antigens through TLR-MyD88 signaling and distinct DC subsets, the IL-17-boosting effect of nasal commensals may be associated with these mechanisms.

We also demonstrated that nasal commensal *S. epidermidis* confers protection against *B. pertussis* infection *in vivo*. Inoculation of mice with *S. epidermidis* before *B. pertussis* challenge showed significantly lowered bacterial burden and tissue damage in the lung. Based on our previous studies, we hypothesized that *S. epidermidis* prevents acute lung infection by enhancing nasal immunity; therefore, we analyzed the immune responses in both nasal and lung tissues following *B. pertussis* infection. In summary, prior administration of *S. epidermidis* promoted an increase in RORγt^+ $CD4^+$ T cells and IL-$17a^+$ cytokine production. This enhancement, occurring primarily in the nasal tissue, may lead to the initial suppression of respiratory pathogen infection, ultimately preventing its invasion into the lungs. Based on these findings, we identified its antimicrobial effects and considered its ability to prevent respiratory pathogen infection using live attenuated vaccines.

The recurrent occurrence of whooping cough despite high vaccination rates is primarily attributed to the problem of waning immunity and short-term effects, where the protective immune response lasts less than 2 years[31]. In addition, the resurgence of whooping cough in adolescents and adults is largely attributed to diminished immunity, serving as a continuous source of infection for unvaccinated or incompletely vaccinated young infants[32]. The establishment of an inappropriate defense system is also largely attributed to the fact that conventional aP vaccination enhances the Th2 response, not the Th1/Th17 response. These issues are recognized as the predominant factors underlying continuous *B. pertussis* infection; therefore, the development of new vaccines is ultimately required to eradicate *B. pertussis* infections. While there have been studies exploring the introduction of new adjuvants and investigating different vaccination routes, such as intranasal administration, to enhance the effectiveness of current aP vaccines, few studies have targeted the development of a new aP vaccine. Thus, in part 2, we aimed to address two issues present in the current aP vaccine by developing a recombinant pertussis protein using the ChaH2 fusion partner and lowering toxicity through genetic mutations, thereby providing a

comprehensive solution. Recent evidence has shown that genetically detoxified toxin induces superior antigen-specific T cell activation and IL-17 polarization compared to chemically detoxified toxin[33]. While the PTX of the current aP vaccine has been chemically detoxified using glutaraldehyde and formaldehyde, we used genetically engineered ChaH2-PtxA^{m}, implying that molecular genetic techniques lead to higher immunogenic properties of the NRaP vaccine. In our results, systemic neutralizing antibodies were highly induced in NRaP-immunized mice. Moreover, our recombinant proteins are cost-effective and enable mass production, which can increase the global vaccination rate. Future studies will be required to investigate the long-term immunogenicity of newly developed subunit aP vaccines and the expansion of antigen specific Trm cells in the respiratory tract, which is necessary to prevent re-infection.

In addition, we conducted experiments to assess whether the use of nasal commensals in immunization methods enhances vaccine immunogenicity. Previous studies have demonstrated the effects of microorganisms as natural adjuvants. For instance, co-administration of oral bacteria with spike protein for intranasal immunization revealed a lower SARS-CoV-2 virus titer compared to intramuscular vaccination alone[34]. Furthermore, one study reported that treating *Bacillus toyonensis*, which is known as a probiotic gut commensal, for five days before subcutaneous vaccination significantly improved humoral immune responses[35]. In contrast to previous studies, our results revealed that stimulating respiratory immunity by respiratory commensals downregulated systemic IgG responses. We attributed this phenomenon to the boosting of airway immune responses, which may have led to a relative decrease in peripheral IgG antibody production induced by intramuscular immunization. Therefore, we hypothesized that intranasal immunization supplemented with nasal commensals could lead to more effective inhibition of respiratory pathogens. This assumption is based on the potential for mucosal immune boosting through nasal commensals and bystander activation of T cells via the stimulation of microbe antigens.

IV. CONCLUSION

Our study elucidates the immunomodulatory effects of the nasal commensal S. *epidermidis* in stimulating the nasal immune system and its antagonistic action against *B. pertussis* during the acute phase of infection, showcasing its antibacterial capabilities. Additionally, we engineered NRaP vaccines that incorporate genetically modified *B. pertussis* virulence factors, resulting in heightened PRN-specific IgG levels and improved immunogenicity over current aP vaccines. Our findings present dual approaches for the prevention of *B. pertussis* infection through the administration of nasal commensals and NRaP vaccination. Despite these advances, the exact mechanisms by which *S. epidermidis* inhibits bacterial infection remain unclear, and further research is necessary to understand the cellular immune responses and the durability of immunity conferred by the NRaP vaccine. Ultimately, our research identifies potential therapeutic avenues for the prevention of respiratory infections caused by various pathogens.

REFERENCES

1. Higgs R, Higgins S, Ross P, Mills K. Immunity to the respiratory pathogen Bordetella pertussis. Mucosal immunology 2012;5:485-500.
2. Melvin JA, Scheller EV, Miller JF, Cotter PA. Bordetella pertussis pathogenesis: current and future challenges. Nature Reviews Microbiology 2014;12:274-88.
3. Carbonetti NH. Immunomodulation in the pathogenesis of Bordetella pertussis infection and disease. Current Opinion in Pharmacology 2007;7:272-8.
4. Solans L, Locht C. The role of mucosal immunity in pertussis. Frontiers in immunology 2019;9:3068.
5. Raeven RH, Brummelman J, Pennings JL, Nijst OE, Kuipers B, Blok LE, et al. Molecular signatures of the evolving immune response in mice following a Bordetella pertussis infection. PloS one 2014;9:e104548.
6. Kroes M, Miranda-Bedate A, Jacobi R, Van Woudenbergh E, Den Hartog G, Van Putten J, et al. Bordetella pertussis-infected innate immune cells drive the anti-pertussis response of human airway epithelium. Scientific Reports 2022;12:3622.
7. Ross PJ, Sutton CE, Higgins S, Allen AC, Walsh K, Misiak A, et al. Relative contribution of Th1 and Th17 cells in adaptive immunity to Bordetella pertussis: towards the rational design of an improved acellular pertussis vaccine. PLoS pathogens 2013;9:e1003264.
8. Misiak A, Wilk MM, Raverdeau M, Mills KH. IL-17–Producing innate and pathogen-specific tissue resident memory γδ T cells expand in the lungs of Bordetella pertussis–infected mice. The Journal of Immunology 2017;198:363-74.
9. Hellwig SM, van Spriel AB, Schellekens JF, Mooi FR, van de Winkel JG. Immunoglobulin A-mediated protection against Bordetella pertussis infection. Infection and immunity 2001;69:4846-50.
10. Wilk MM, Misiak A, McManus RM, Allen AC, Lynch MA, Mills KH. Lung CD4 tissue-resident memory T cells mediate adaptive immunity induced by previous infection of mice with Bordetella pertussis. The Journal of Immunology 2017;199:233-43.
11. Alghounaim M, Alsaffar Z, Alfraij A, Bin-Hasan S, Hussain E. Whole-cell and acellular pertussis vaccine: reflections on efficacy. Medical Principles and Practice 2022;31:313-21.
12. Szwejser-Zawislak E, Wilk MM, Piszczek P, Krawczyk J, Wilczyńska D, Hozbor D. Evaluation of Whole-Cell and Acellular Pertussis Vaccines in the Context of Long-Term Herd Immunity. Vaccines 2022;11:1.
13. da Silva Antunes R, Babor M, Carpenter C, Khalil N, Cortese M, Mentzer AJ, et al. Th1/Th17 polarization persists following whole-cell pertussis vaccination despite repeated acellular boosters. J Clin Invest 2018;128:3853-65.
14. Warfel JM, Zimmerman LI, Merkel TJ. Acellular pertussis vaccines protect against disease but fail to prevent infection and transmission in a nonhuman primate model. Proceedings of the National Academy of Sciences 2014;111:787-92.
15. Diavatopoulos DA, Edwards KM. What is wrong with pertussis vaccine immunity? Why immunological memory to pertussis is failing. Cold Spring Harbor Perspectives in Biology 2017;9:a029553.
16. Bottero D, Gaillard ME, Fingermann M, Weltman G, Fernández J, Sisti F, et al. Pulsed-field gel electrophoresis, pertactin, pertussis toxin S1 subunit polymorphisms, and surfaceome analysis of vaccine and clinical Bordetella pertussis strains. Clinical and

Vaccine Immunology 2007;14:1490-8.
17. Williams MM, Sen K, Weigand MR, Skoff TH, Cunningham VA, Halse TA, et al. Bordetella pertussis strain lacking pertactin and pertussis toxin. Emerging infectious diseases 2016;22:319.
18. Golebski K, Hoepel W, Van Egmond D, De Groot E, Amatngalim G, Beekman J, et al. FcγRIII stimulation breaks the tolerance of human nasal epithelial cells to bacteria through cross-talk with TLR4. Mucosal immunology 2019;12:425-33.
19. Clark SE. Commensal bacteria in the upper respiratory tract regulate susceptibility to infection. Curr Opin Immunol 2020;66:42-9.
20. Man WH, de Steenhuijsen Piters WA, Bogaert D. The microbiota of the respiratory tract: gatekeeper to respiratory health. Nature Reviews Microbiology 2017;15:259-70.
21. Merenstein C, Bushman FD, Collman RG. Alterations in the respiratory tract microbiome in COVID-19: current observations and potential significance. Microbiome 2022;10:165.
22. Liu Q, Liu Q, Meng H, Lv H, Liu Y, Liu J, et al. Staphylococcus epidermidis Contributes to Healthy Maturation of the Nasal Microbiome by Stimulating Antimicrobial Peptide Production. Cell Host Microbe 2020;27:68-78 e5.
23. Kim HJ, Jo A, Jeon YJ, An S, Lee KM, Yoon SS, et al. Nasal commensal Staphylococcus epidermidis enhances interferon-lambda-dependent immunity against influenza virus. Microbiome 2019;7:80.
24. Naik S, Bouladoux N, Linehan JL, Han S-J, Harrison OJ, Wilhelm C, et al. Commensal–dendritic-cell interaction specifies a unique protective skin immune signature. Nature 2015;520:104-8.
25. Li H, Cao L, Zhang Y, Ren H, Zhao P, Xu W. Human respiratory syncytial virus F protein expressed in Pichia pastoris or Escherichia coli induces protective immunity without inducing enhanced respiratory disease in mice. Archives of Virology 2020;165:1057-67.
26. Deng Y, Chen W, Zang N, Li S, Luo Y, Ni K, et al. The antiasthma effect of neonatal BCG vaccination does not depend on the Th17/Th1 but IL-17/IFN-γ balance in a BALB/c mouse asthma model. Journal of clinical immunology 2011;31:419-29.
27. Hall OJ, Limjunyawong N, Vermillion MS, Robinson DP, Wohlgemuth N, Pekosz A, et al. Progesterone-based therapy protects against influenza by promoting lung repair and recovery in females. PLoS pathogens 2016;12:e1005840.
28. Li Y, Wang W, Yang F, Xu Y, Feng C, Zhao Y. The regulatory roles of neutrophils in adaptive immunity. Cell Communication and Signaling 2019;17:1-11.
29. Yang D, Chen X, Wang J, Lou Q, Lou Y, Li L, et al. Dysregulated lung commensal bacteria drive interleukin-17B production to promote pulmonary fibrosis through their outer membrane vesicles. Immunity 2019;50:692-706. e7.
30. Naik S, Bouladoux N, Wilhelm C, Molloy MJ, Salcedo R, Kastenmuller W, et al. Compartmentalized control of skin immunity by resident commensals. Science 2012;337:1115-9.
31. Damron FH, Barbier M, Dubey P, Edwards KM, Gu X-X, Klein NP, et al. Overcoming waning immunity in pertussis vaccines: workshop of the National Institute of Allergy and Infectious Diseases. The Journal of Immunology 2020;205:877-82.
32. Tozzi AE, Celentano LP, degli Atti MLC, Salmaso S. Diagnosis and management of pertussis. Cmaj 2005;172:509-15.
33. Surendran N, Pichichero M. Genetically detoxified pertussis toxin induces superior antigen specific CD4 T cell responses compared to chemically detoxified pertussis toxin. Human Vaccines & Immunotherapeutics 2019;15:1167-70.

34. Nagai M, Moriyama M, Ichinohe T. Oral bacteria combined with an intranasal vaccine protect from influenza A Virus and SARS-CoV-2 Infection. Mbio 2021;12:10.1128/mbio.01598-21.
35. Santos F, Ferreira M, Maubrigades L, Gonçalves V, de Lara A, Moreira C, et al. Bacillus toyonensis BCT-7112T transient supplementation improves vaccine efficacy in ewes vaccinated against Clostridium perfringens epsilon toxin. Journal of Applied Microbiology 2021;130:699-706.

ABSTRACT(IN KOREAN)

비강 내 공생 미생물을 통한 호흡기 면역 증진 및 새로운 서브 유닛 백신 개발을 통한 백일해 감염 억제 연구

<지도교수 권호근>

연세대학교 대학원 의과학과

김다정

백일해 균은 호흡기 질환을 유발하는 전염성이 강한 기회 감염균으로 폐의 상피에 결합하여 독소를 분비하며 주변 면역 세포들을 자극한다. 1940년대에는 백일해 균 전 세포 사백신이 개발되었지만, 독성이 강하다는 단점이 있어 이를 개선하고자 백일해 주요 항원인 Pertussis toxin, Filamentous hemagglutinin, Pertactin을 표적화한 백신이 개발되었다. 하지만 이는 백일해 균의 주요 T 도움 1/17 세포 (Th1/Th17)의 분화 보다는 T 도움 2 세포 (Th2)의 면역 반응이 증진되어 접종 후에도 백일해 균이 폐에 높게 검출된다는 한계가 있다. 또한, 백신 접종 후에도 방어 면역이 2년 이상 지속되지 못한다는 점에서 높은 백신 접종률에도 백일해가 반복하여 발생한다. 따라서, 백일해 감염이 지속하는 현 시점에서 본 연구에서는 두 가지 전략을 통해 호흡기 감염으로부터 예방하고자 한다. 비강 내 공생 미생물이 호흡기 면역을 증진시키며 백일해 균의 감염이 급성 감염 시기에 억제되는 것을 확인하였다. 또한 대장균에서

유래한 새로운 재조합 단백질 백일해 백신 개발을 통해 상용화되는 백신의 낮은 면역원성의 한계를 극복하고자 했고, 증진된 백신 면역원성을 백일해 감염 마우스 모델을 통해 검증하였다. 이를 통해 백일해 감염 뿐만 아니라 호흡기 감염을 억제할 수 있는 적절한 모델로 활용될 수 있을 것이다.

핵심 되는 말 : 호흡기 면역, 백신, 호흡기 감염, 비강 내 공생 미생물